Laser Mass Ablation Efficiency Measurements Indicate Bubble-Driven Dynamics Dominates Laser Thrombolysis

Robert P. Godwin[a], E. J. Chapyak[a], Scott A. Prahl[b], and HanQun Shangguan[b]

[a]Applied Theoretical and Computational Physics Division, Los Alamos National Laboratory, MS F664, Los Alamos, NM 87545

[b]Oregon Medical Laser Center, Providence St. Vincent Hospital, Portland, OR 97225

ABSTRACT

Mass removal experiments have been performed at the Oregon Medical Laser Center with 10 to 100 mJ 1 μs laser pulses at optical wavelengths. Above the energy threshold for bubble formation, the laser mass ablation efficiency (μg/mJ) for removal of gel surrogate thrombus is nearly constant for a given experimental geometry and gel absorption coefficient. The efficiency in "contact" experiments, in which the optical fiber delivering the energy is in close proximity to the absorbing gel, is approximately three times that of "non-contact" experiments, in which the optical fiber is ~1 mm from the gel. Mass removal occurs hundreds of microseconds after the laser deposition. Experimental data and numerical simulations are consistent with the hypothesis that jet formation during bubble collapse plays a dominant role in mass removal. This hypothesis suggests a model in which the mass removed scales linearly with the maximum bubble volume and explains the distinctive features, including the magnitude, of the mass removal.

Keywords: bubble dynamics, cavitation, hydrodynamics, jet formation, laser thrombolysis, mass ablation efficiency

1. INTRODUCTION

Measurements of the mass ablation efficiency of laser thrombolysis and the dynamics of laser-assisted drug delivery have been performed at the Oregon Medical Laser Center (OMLC).[1-3] These experiments addressed:

1) mass ablation threshold exposures,
2) vapor bubble formation and associated dynamics, and
3) mass ablation efficiency as a function of laser pulse parameters, clot or clot surrogate properties, and experimental geometry. We focus this data analysis on the mass ablation efficiency defined as the clot or gel mass removed per unit energy (μg/mJ).

The OMLC experiments conclusively demonstrate that the mass ablation threshold laser exposures correspond to the threshold for bubble creation. They indicate that bubble formation and associated delayed bubble-driven hydrodynamics dominate both laser thrombolysis mass removal and laser-assisted dynamic drug delivery. We suggest bubble collapse jet dynamics as a paradigm for laser-initiated mass ablation and show that this paradigm is consistent with the principal OMLC experimental findings.

2. MASS ABLATION MEASUREMENTS

In the mass removal experiments, 10 to 100 mJ 1 μs laser pulses at optical wavelengths were delivered through 300 to 1000 μm core diameter quartz fibers to surrogate clot consisting of dyed gelatin or to real clot. (We concentrate on the gelatin experiments because they provide an extensive data set. Clot experiments yield a higher ablation efficiency than do gel experiments by a factor of two to three, but otherwise similar data.) Various geometries were used in the mass ablation and drug delivery experiments, but Fig. 1 is typical. The figure illustrates a "non-contact" experiment, in which the optical fiber delivering the energy is ~1 mm from the gel. In "contact" experiments the fiber is in close proximity to the absorbing gel. Since the ablated gel mass was in a liquid solution, the absorptance of that solution was compared with a calibrated standard dye solution to determine the mass ablated. This spectrophotometric mass measurement was accurate and reproducible with an estimated error of <5%.

R. P. G. (correspondence): Email: rpg@lanl.gov

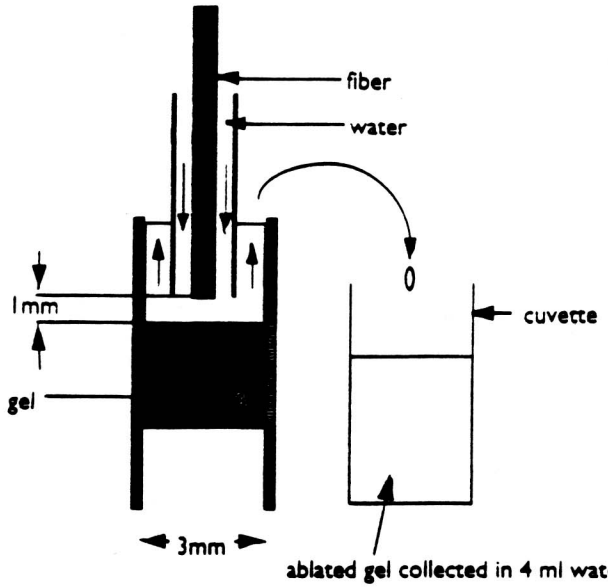

Figure 1. Laser pulses are delivered through a glass fiber to dyed gelatin surrogate clot under water. Ablated gel is collected in water and the absorption measured to determine the mass removed. (Sathyam Ref.1.)

The ablation of gelatin could be observed visibly and was invariably accompanied by an audible snap corresponding to the sound emission expected from the dynamics of a ~1 mm radius bubble.[9,10] No acoustic signals were detected below the threshold for gelatin ablation. The threshold conditions determined by the onset of an audible snap and by several other diagnostics of bubble formation quantitatively agree.

We will demonstrate that the high ablation mass relative to the directly vaporized mass and other experimental features strongly suggest that fluid mechanical action resulting from vapor bubble collapse dominates over other potential ablation processes.

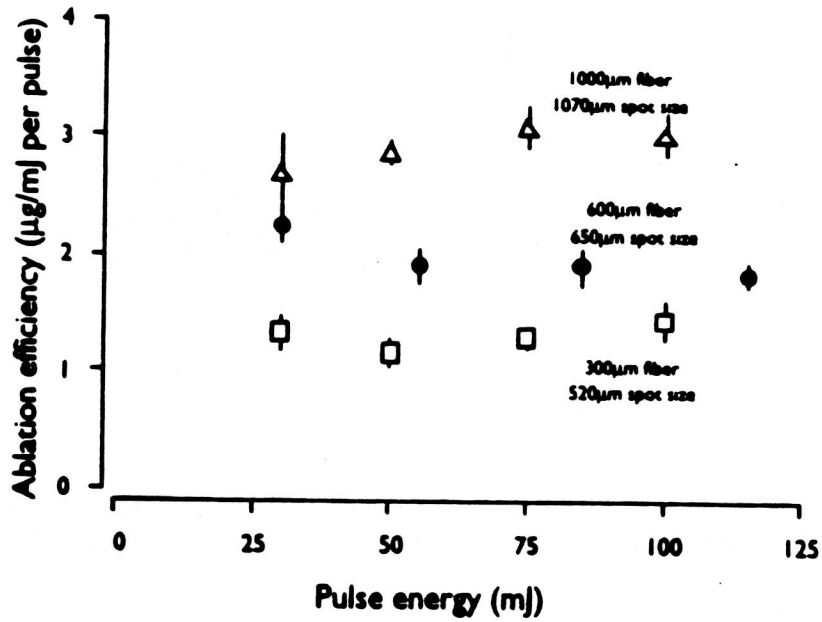

Figure 2. Mass ablation efficiency at various pulse energies and spot sizes. The absorption coefficient of the gelatin was 300 cm^{-1}. Above the threshold for bubble formation, the mass ablation efficiency is sensibly constant. Other experiments show the ablation efficiency is independent of gel absorption above the bubble formation threshold. (Sathyam Ref.1.)

Define the following efficiencies:

$\varepsilon_{AL} \equiv$ laser mass ablation efficiency $= m_A / E_L$,

$\varepsilon_{BL} \equiv$ efficiency for conversion of laser to bubble energy $= E_B / E_L$, and

$\varepsilon_{AB} \equiv$ bubble mass ablation efficiency $= m_A / E_B$;

where m_A(μg) is the mass ablated, E_L(mJ) the incident laser pulse energy, and E_B(mJ) the PdV energy stored in the laser-produced bubble at its maximum radius.

As Fig. 2. demonstrates, once the laser energy delivered to the target gel exceeds the threshold for bubble formation, the mass removal efficiency is essentially constant at 2 to 3 μg/mJ in "non-contact" experiments.[1] The mass removed is linearly related to the total energy delivered (*not* to the energy/area) and to the energy stored in the bubble formed. For a given experimental geometry and absorption coefficient, the mass ablation efficiency is nearly constant above the threshold pulse energy. The ablation efficiency is relatively insensitive to the area of deposition and laser wavelength. In these particular experiments the efficiency for conversion of laser to bubble energy is <5%.

Photographic records demonstrate that the ejection of target material (that is, gel or clot) begins after the growth and collapse of the bubble and continues over an extended period. Reproducing this late mass ejection is a key element of a successful ablation model. Delayed mass removal is a feature likely to be difficult to duplicate with numerical simulations without a fundamental understanding of its origins. In the experimental series depicted in Fig. 3., a 50 mJ laser pulse has created a bubble of maximum diameter ~3 mm with growth and collapse times both ~150 μs. Gelatin ablation begins at ~300 μs and continues for an extended period.

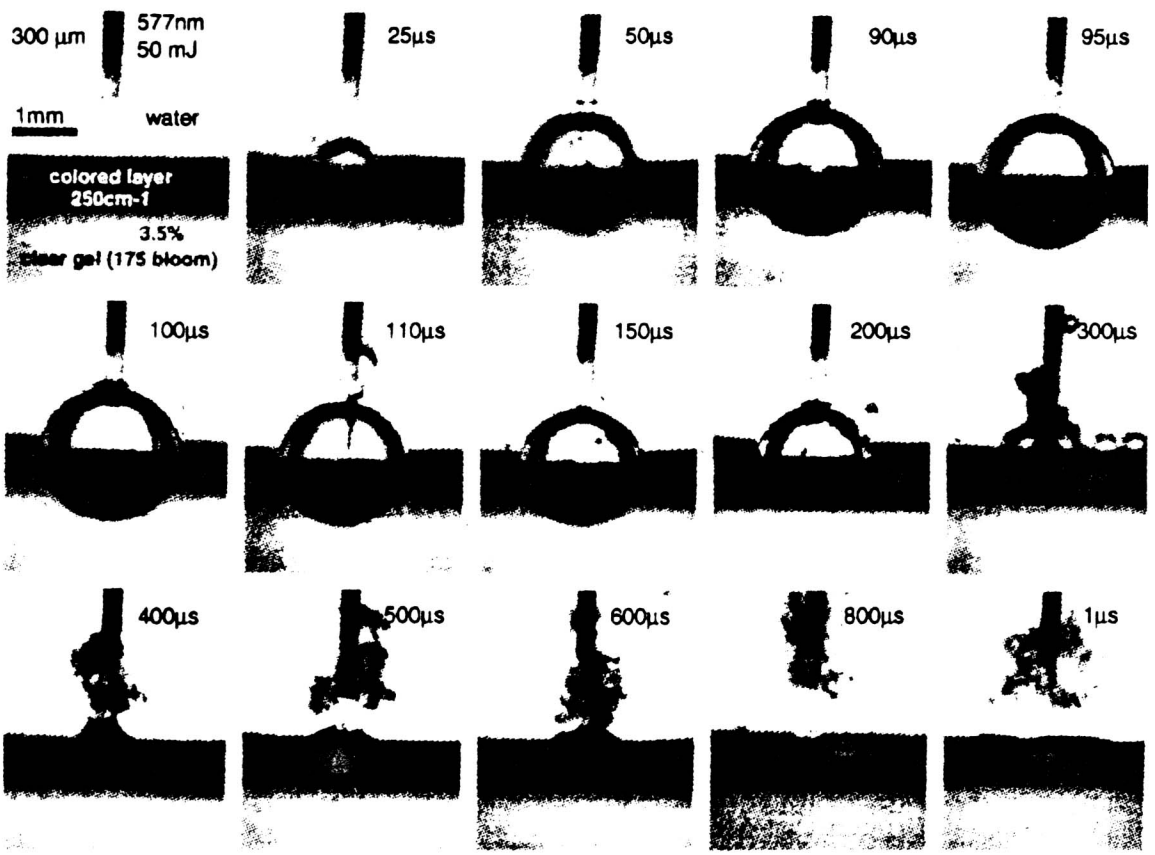

Figure 3. Flash photographs in side view of bubble growth and collapse after delivery of a 50 mJ 1 μs laser pulse to dyed gelatin under water. The frames were taken on different experiments, but with nominally the same conditions. The maximum bubble radius and collapse occur near the times expected for an isolated Rayleigh bubble of 1.6 mm radius. The volcanolike upward ejection of gelatin mass begins upon bubble collapse. (Shangguan OMLC.)

We hypothesize that bubble-driven dynamics produces laser mass ablation. We therefore concentrate our analysis on bubble-driven mass ablation in our search for a paradigm of laser-driven ablation. From the Sathyam OMLC experiments in which <5% of the laser energy was stored as bubble energy, we infer a bubble mass ablation efficiency

$$\varepsilon_{AB} = \frac{m_A}{E_B} = \frac{m_A}{E_L}\cdot\frac{E_L}{E_B} = \frac{\varepsilon_{AL}}{\varepsilon_{BL}} > 3\frac{\mu g}{\text{mJ}}\cdot\frac{1}{5\times10^{-2}} = 60\frac{\mu g}{\text{mJ}}. \quad (1)$$

For comparison, the efficiency for vaporization of water at 100°C is

$$\varepsilon_V \equiv L_V^{-1} = (2.25\times10^3\ \text{J/g})^{-1} = 0.41\ \mu\text{g/mJ}, \quad (2)$$

where L_V is the latent heat of vaporization. The ratio of the measured ablation efficiency to the efficiency for water vaporization, $\varepsilon_{AL}/\varepsilon_V \approx 3/0.4 \approx 8$, is large especially when one considers the low conversion efficiency of laser energy to bubble energy. The high bubble mass ablation efficiency is responsible for the large $\varepsilon_{AL}/\varepsilon_V$ ratio. Understanding the bubble mass ablation efficiency is thus necessary for understanding and optimizing laser thrombolysis.

3. HYDRODYNAMIC ESSENTIALS

The energy stored in a bubble of maximum radius R_o in a fluid of pressure P_o is

$$E_B = P_o V_o = P_o\frac{4}{3}\pi R_o^3 = \rho\frac{4}{3}\pi R_o^3 v_o^2. \quad (3)$$

The characteristic bubble collapse velocity, $v_o \equiv \sqrt{P_o/\rho}$, is 10 m/s for water at atmospheric pressure (1 atm ≈ 1 bar = 10^6 dynes/cm^2 = 0.1 MPa). The associated Rayleigh cavity collapse time $\tau(\mu s) = 91.5\,R_o(\text{mm})$ for a bubble in water.[11-13] The effective fluid mass associated with the bubble dynamics is $m_{eB} = \rho\,4\pi R_o^3$ and three times the mass missing due to the bubble cavity.

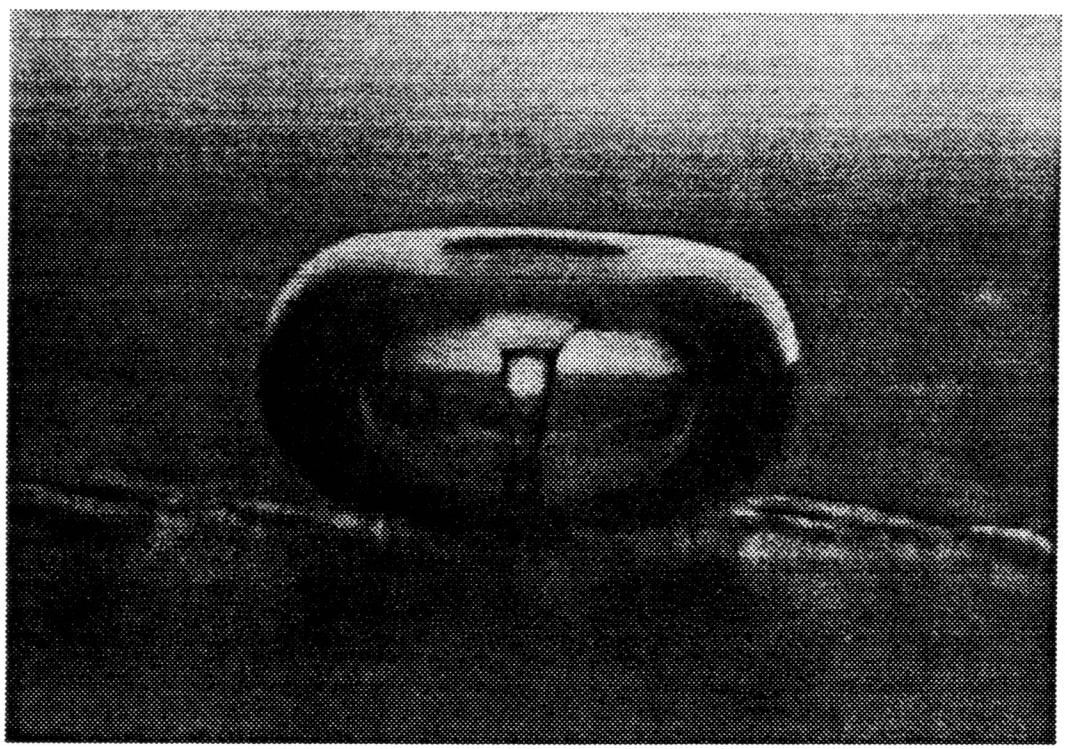

Figure 4. Bubble collapse onto a wall with the formation of a wallward jet. The jet can be roughly approximated by a cylinder with a radius of one-tenth the 2 mm maximum bubble radius and a length comparable to that radius. This dramatic and often-reproduced photo is familiar to the bubble dynamics research community. (Courtesy of L. A. Crum.)

Bubbles collapsing near walls and near free surfaces produce strong jetting normal to the interfaces. The experimental, theoretical, and computational study of bubbles and of fluid jets are mature, but still vigorous, fields of applied physics. Studies of marine propellor sounds and cavitation damage and the development of explosively-formed armor-piercing munitions were important in providing the scientific foundations of bubble and jet dynamics.[14,15] Figure 4 is a dramatic photo of a bubble collapse jet onto a wall which has become famous in the bubble dynamics research community.[16] Figure 5 demonstrates the capability of the Los Alamos MESA-2D Eulerian hydrodynamics code to model a similar situation. MESA-2D simulations agree with classic calculations and experimental measurements of bubble-collapse jetting near both walls and free surfaces.[17,18] Eulerian numerical hydrodynamics is particularly effective for modeling very distorted flows such as those leading to jet formation. See Ref. 10 for the physical and numerical details of the test problem setup.

We approximate and parameterize a jet as an equivalent right circular cylinder of fluid with a constant velocity $v_j = \alpha v_o$, radius $r_j = \beta R_o$, and length $l_j = \gamma R_o$. The scale factors α, β, and γ relate the characteristic bubble wall velocity, v_o, and maximum bubble radius, R_o, to the jet parameters. Jets with $\alpha \leq 10$, $\beta \sim 0.1$, and $\gamma \sim 1$ are common features of bubble dynamics in a variety of situations.[14]

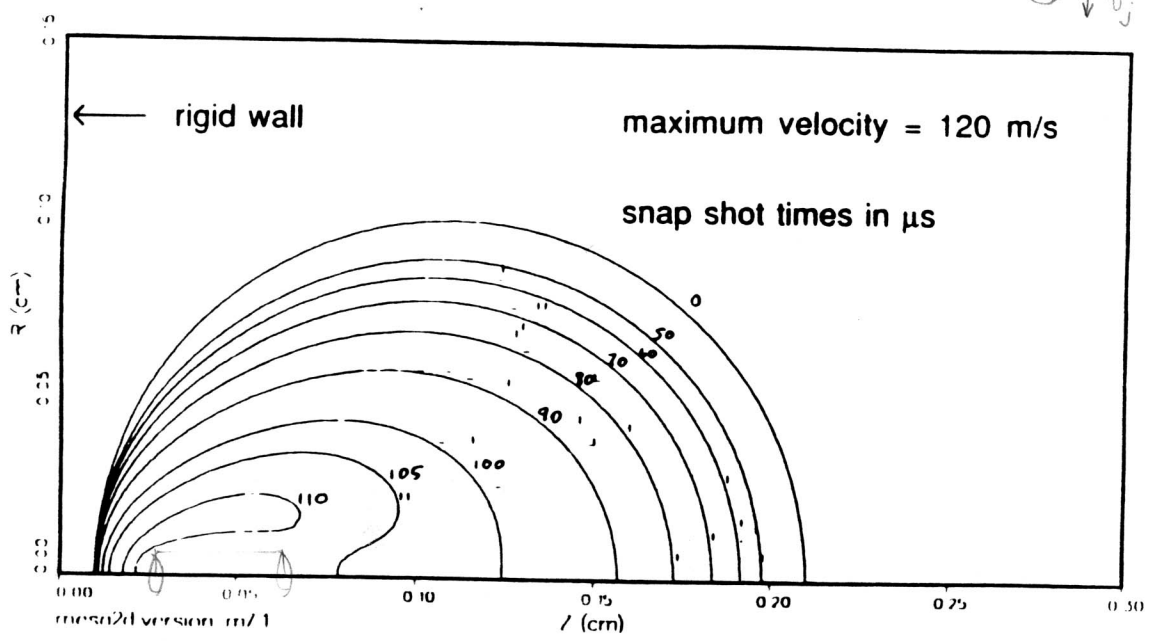

Figure 5. Numerical snapshots of the collapse of an initially spherical water cavity containing a low-pressure perfect gas simulated with the bubble center located 1.1 radii from a perfectly-rigid wall. Times are in microseconds. The simulation was performed as a computational test validating Los Alamos numerical tools for modeling bubble dynamics. The MESA-2D code produces a jet with scaling parameters $\alpha \approx 12$, $\beta \sim 0.1$, and $\gamma \sim 0.5$.

4. JET DYNAMICS AS A THROMBOLYSIS PARADIGM

With the exception of the optical fiber and catheter, the materials and tissues in the neighborhood of laser thrombolysis bubbles have the density of water. Assume they behave as inviscid incompressible fluids. Fluid behavior dominates when driving pressures greatly exceed material strengths. In thrombolysis, fluid pressures near the bubble reach many atmospheres and the Young's modulus of clot and gel is ~20 kPa = 0.2 bar easily satisfying the criterion for dynamic fluid behavior. (That evolution produced a clot Young's modulus of this magnitude is not surprising, since the systolic blood pressure is ≤140 mm Hg ≈ 0.2 bar.)

With our parameterization, we expect a bubble collapse jet mass

$$m_j = \rho A_j l_j = \beta^2 \gamma \rho \pi R_o^3 = \frac{3}{4}\beta^2 \gamma \cdot \frac{E_B}{v_o^2}. \tag{4}$$

We hypothesize that the mass of a bubble collapse jet can be equated to the laser-ablated mass. This *Ansatz* suggests a bubble mass ablation efficiency

$$\varepsilon_{AB} = \frac{m_j}{E_B} = \frac{3}{4}\frac{\beta^2 \gamma}{v_o^2} = 7.5 \times 10^3 \beta^2 \gamma \frac{\mu g}{\text{mJ}}, \tag{5}$$

since $v_o^2 = P_o / \rho = 10^6$ (cm/s)^2 = 10^{-4} mJ/μg. This efficiency has no variables! As long as a bubble is created and that bubble leads to a jet whose dimensions scale with those of the bubble, the efficiency of mass removal is constant if our jet dynamics hypothesis is correct. Of course, the total mass removal scales as R_o^3 and therefore linearly with the bubble energy and with the incident laser pulse energy. With the scaling parameters $\beta \sim 0.1$ and $\gamma \sim 1$, we estimate $\varepsilon_{AB} \sim 75\,\mu$g/mJ, in qualitative agreement with the value inferred above from OMLC's measurements. We can similarly define jet mass and kinetic energy efficiencies as

$$\varepsilon_{Mj} \equiv m_j / m_{eB} = \beta^2 \gamma / 4 \tag{6}$$

and

$$\varepsilon_{KEj} \equiv KE_j / E_B = \alpha^2 \beta^2 \gamma / 24 \tag{7}$$

respectively; $\varepsilon_{Mj} \sim 2 \times 10^{-3}$ and $\varepsilon_{KEj} \sim 4 \times 10^{-2}$ are typical. The energy expended in overcoming strength effects in the gel or clot mass so that it will behave as a fluid in the bubble neighborhood is $E_f \sim Y\, m_{eB}/\rho = Y\, 4\pi\, R_o^3$, where Y is the nominal strength of the gel or clot. With $Y \sim 0.2$ bar and $R_o \sim 1$ mm, $E_f \sim 2$ mJ which is comparable to the bubble energy $E_B = \varepsilon_{BL} E_L$. To lyse or breakup the mass removed in thrombolysis will require an additional energy of only $\varepsilon_{Mj} E_f \sim \mu$J.

An enhancement factor of about three in the mass ablation efficiency of "contact" compared to "non-contact" thrombolysis experiments is measured. This observation further supports the jet dynamics paradigm as shown by the following qualitative discussion.

A bubble collapsing near a rigid wall forms a wallward jet.[14,17] Considering the flow to be inviscid and incompressible allows this situation to be modeled using the method of images. A single bubble collapse near a wall is thus mathematically equivalent to the collapse of two identical bubbles separated by twice the bubble-wall distance. There is, however, only half as much energy invested in hydrodynamic motion in the bubble-wall case as in the "equivalent" two-bubble situation.

The collapse of a bubble near a fluid free surface produces a pair of jets moving away from the surface; one into the fluid and one into the void.[14,18] Using the method of images suggests the jet into the fluid. The second jet into the void is required to satisfy the conservation of axial momentum. In the case of bubble collapse near a wall, the massive wall satisfies the conservation of momentum, and no second jet is required. The dynamics of a bubble in the neighborhood of a compliant surface is intermediate between the rigid-wall and free-surface cases and is a strong function of the compliant material's properties.[19]

If the axial optical fiber influences the dynamics in the "contact" thrombolysis experiments in a manner similar to that of a wall, the fiber may provide a factor of up to two increase in the jet dynamic energy for ablation because the energy expended in fluid flow in one-half space is spared. Further, if the axial fiber influence is sufficiently like that of a wall, it will allow the conservation of momentum to be satisfied with only one jet in the case of "contact" experiments, whereas a pair of oppositely directed jets will be required in "non-contact" experiments. Thus momentum conservation may provide up to another factor of two enhancement in ablation efficiency. One might assume an optical fiber with a diameter significantly greater than the maximum bubble diameter would be required for the fiber effects on dynamics to approach those of an ideal wall. However, bubble collapse jets typically have a diameter of order one-tenth the maximum bubble diameter. As a result, axial momentum conservation can be achieved in "contact" experiments with a fiber diameter significantly smaller than the maximum bubble diameter as long as the jet diameter is less than the fiber diameter. In the OMLC experiments the bubbles, fibers, and jets have typical diameters of 3, ≥0.3, and 0.2 mm respectively and thus satisfy the required criterion. Jet dynamics explains a "contact" ablation enhancement of more than a factor of two relative to "non-contact" ablation. Numerical simulations can provide quantitative estimates of the mass ablation efficiency effects of fiber proximity on bubble collapse jet dynamics and parameter studies for understanding

and optimizing the late-time bubble-driven mass removal dynamics. The MESA-2D code has been validated with test problems for modeling bubble dynamics and associated jetting, and numerical studies of bubbles at a material interface similar to those in thrombolysis experiments exhibit dramatic jet dynamics. [10,20]

5. CONCLUSIONS

Considering the approximate nature of our analysis, the agreement of the suggested bubble collapse jet dynamics paradigm with important features of laser thrombolysis mass ablation experiments is excellent. The paradigm successfully explains the magnitude and constancy of the measured ablation efficiency. It also explains the late mass removal dynamics and why the ablation efficiency is higher in "contact" experiments than in "non-contact" experiments. This broad agreement with observations indicates that bubble-driven jet formation, or other closely related fluid dynamics which scales linearly with bubble energy, is a suitable paradigm for clot mass removal in laser thrombolysis. Despite its successes, our heuristic jet model provides no detailed information on the actual mass removal process. It does not even predict the expected direction of jets at the clot-fluid interface or suggest the details of material failure. We are employing two-dimensional simulations in cylindrical symmetry using computational tools capable of reliably modeling severely distorted flows to investigate the jet mass removal paradigm as a function of various parameters and material properties in realistic thrombolysis scenarios.[21] With sufficiently fine temporal and spatial zoning, these studies offer the promise of identifying and optimizing the details of the jetting or jetlike behavior that our analysis indicates is the dominant laser thrombolysis mass removal mechanism. We expect the jet mass removal paradigm to be valid for certain other laser and ultrasonic medical procedures in which bubbles drive soft-tissue dynamics.

6. ACKNOWLEDGMENTS

This work was supported in part by a Cooperative Research and Development Agreement (CRADA) between Los Alamos National Laboratory (Department of Energy), Oregon Medical Laser Center, and Palomar Medical Technologies.

7. REFERENCES

1. U. S. Sathyam, "Laser Thrombolysis: Basic Ablation Studies," Ph.D. thesis, Oregon Graduate Institute of Science and Technology, 1996.

2. U. S. Sathyam, A. Shearin, and S. A. Prahl, "Visualization of Microsecond Laser Ablation of Porcine Clot and Gelatin Under a Clear Liquid," *Lasers in Surgery: Advanced Characterization, Therapeutics, and Systems VII, Proc. SPIE*, **2671**, pp. 28-35, 1996.

3. U. S. Sathyam, A. Shearin, E. A. Chasteney, and S. A. Prahl, "Threshold and ablation efficiency studies of microsecond ablation of gelatin under water," *Lasers Surg. Med.*, **19**, pp. 397-406, 1996.

4. U. S. Sathyam, A. Shearin, and S. A. Prahl, "Investigations of Basic Ablation Phenomena During Laser Thrombolysis," *Lasers in Surgery: Advanced Characterization, Therapeutics, and Systems VII, Proc. SPIE*, **2970**, pp. 19-27, 1997.

5. H. Shangguan, "Local Drug Delivery with Microsecond Laser Pulses: *In Vitro* Studies," Ph.D. thesis, Portland State University, 1996.

6. H. Shangguan, L. W. Casperson, and S. A. Prahl, "Microsecond Laser Ablation of Thrombus and Gelatin under Clear Liquids: Contact vs. Non-contact," *IEEE J. Selected Topics Quantum Electron.*, **2**, pp. 818-825, 1996.

7. H. Shangguan, L. W. Casperson, and S. A. Prahl, "Effects of Laser Delivery on Ablation Efficacy of Thrombus in Liquids: In Vitro Study," *Lasers Surg. Med.*, **S9**, pp. 818-825, 1996.

8. H. Shangguan, L. W. Casperson, K. W. Gregory, and S. A. Prahl, "Penetration of Fluorescent Particles in Gelatin During Laser Thrombolysis," *Lasers in Surgery: Advanced Characterization, Therapeutics, and Systems VII, Proc. SPIE*, **2970**, pp. 10-18, 1997.

9. L. D. Landau and E. M. Lifshitz, Sec. 73, "Emission of Sound," **Fluid Mechanics**, Pergamon, Oxford, 1959.

10. E. J. Chapyak and R. P. Godwin, "Numerical studies of bubbles in laser thrombolysis," *in Lasers in Surgery: Advanced Characterization, Therapeutics, and Systems VI*, R. Rox Anderson, M.D., Editor, Proc. SPIE **2671**, pp. 84-87 (1996).

11. Lord Rayleigh, "On the pressure developed in a liquid during the collapse of a spherical cavity," *Phil. Mag.* **34**, pp. 94-98, 1917.

12. L. D. Landau and E. M. Lifshitz, Chap. 1, "Ideal Fluids," Prob. 7, **Fluid Mechanics**, Pergamon, Oxford, 1959.

13. J. Lighthill, Chap. 7, "Three-dimensional examples of irrotational flows," **An Informal Introduction to Theoretical Fluid Mechanics**, Claredon, Oxford, 1986.

14. F. R. Young, Sec. 3.8 "High speed photographic studies of bubble motion" and Sec. 4.13.3 "Physical mechanisms that cause cavitation erosion," **Cavitation**, McGraw Hill, London, 1989.

15. G. D. Birkhoff, D. MacDougall, E. Pugh, and G. Taylor, "Explosives with Lined Cavities," *J. Appl. Phys.*, 19(6), pp. 563-582, (1948).

16. L. A. Crum,"Surface Oscillations and Jet Development in Pulsating Air Bubbles," *J. de Physique Colloque*, **40** (C8), pp. 285-288 (1979). The photograph has been frequently reprinted. It appears, for example, in Ref. 14.

17. M. A. Plesset and R. B. Chapman, "Collapse of an initially spherical vapour cavity in the neighborhood of a solid boundary," *J. Fluid Mech.*, **47**, pp. 283-290, 1971.

18. G. L. Chahine, "Interaction Between an Oscillating Bubble and a Free Surface," *Trans. ASME, J. Fluids Engng.*, **99**, pp. 709-716, 1977.

19. A. Shima, Y. Tomita, D. C. Gibson, and J. R. Blake, "The growth and collapse of cavitation bubbles near composite surfaces," *J. Fluid. Mech.*, **203**, pp. 199-214, 1989.

20. E. J. Chapyak, R. P. Godwin, S. A. Prahl, and H. Shangguan, "A Comparison of Numerical Simulations and Laboratory Studies of Laser Thrombolysis," *Lasers in Surgery: Advanced Characterization, Therapeutics, and Systems VII, Proc. SPIE*, **2970**, pp. 28-34, 1997.

21. E. J. Chapyak and R. P. Godwin, "Physical Mechanisms of Importance to Laser Thrombolysis," *Lasers in Surgery: Advanced Characterization, Therapeutics, and Systems VIII, Proc. SPIE*, **3245**, 1998 (to be published).